Journal of Zhejiang University-SCIENCE C (Computers & Electronics)
ISSN 1869-1951 (Print); ISSN 1869-196X (Online)
www.zju.edu.cn/jzus; www.springerlink.com
E-mail: jzus@zju.edu.cn

Improving the real-time performance of Ethernet for plant automation (EPA) based industrial networks*

Li LU[†1,2], Dong-qin FENG[†‡1,2], Jian CHU[1,2]

([1]*Institute of Cyber-Systems and Control, Zhejiang University, Hangzhou 310027, China*)

([2]*State Key Laboratory of Industrial Control Technology, Zhejiang University, Hangzhou 310027, China*)

[†]E-mail: {llu, dqfeng}@iipc.zju.edu.cn

Received Dec. 19, 2012; Revision accepted Apr. 23, 2013; Crosschecked May 17, 2013

Abstract: Real-time Ethernet (RTE) control systems with critical real-time requirements are called fast real-time (FRT) systems. To improve the real-time performance of Ethernet for plant automation (EPA), we propose an EPA-FRT scheme. The minimum macrocycle of EPA networks is reduced by redefining the EPA network frame format, and the synchronization process is modified to acquire higher accuracy. A multi-segmented topology with a scheduling scheme is introduced to increase effective bandwidth utilization and reduce protocol overheads, and thus to shorten the communication cycle significantly. Performance analysis and practical tests on a prototype system show the effectiveness of the proposed scheme, which achieves the best performance at small periodic payload in large scale systems.

Key words: Ethernet for plant automation (EPA), Fast real-time (FRT) system, Real-time Ethernet (RTE), Scheduling scheme
doi:10.1631/jzus.C1200363 **Document code:** A **CLC number:** TP293

1 Introduction

Ethernet has been the dominant network communication standard in home and office use in recent decades. As a distributed communication system, Ethernet is fast, efficient, cheap, and easy to use and maintain, offering an attractive choice for use in industrial areas (Sauter and Vasques, 2006; Hespanha *et al*., 2007; Sauter, 2010).

The full-duplex switched Ethernet can avoid the collisions introduced by carrier sense multiple access with collision detection (CSMA/CD) (IEEE802.3: 2005) in the media access control (MAC) layer. Additionally, the upper bound of transmission latency should be restricted to a deterministic value by some queue management policies in the switches. The delay introduced by switches, however, can hardly meet the timing requirements in the so-called hard real-time system unless the switch is specially designed. As an example, High Speed Ethernet (HSE) (FF-581:2003) defined in IEC 61158 (IEC-61158-3, 4, 5, 6:2000) based on switched Ethernet is usually used in higher levels of automation hierarchy instead of the field level. Generally speaking, the common Ethernet must be modified in the MAC layer or data link layer (DLL) to achieve deterministic communications and to be applicable to industrial areas, especially in fast motion control scenarios (Felser, 2005).

Major efforts have been dedicated to the research and standardization of industrial Ethernet protocols, and the conception of real-time Ethernet (RTE) (Decotignie, 2005) has been widely accepted recently. Many automation manufacturers have put forward their own Ethernet based Fieldbus protocols, e.g., PROFINET Powerlink, EtherCAT, and EPA (IEC-61784-14:2007). The EPA protocol is designed essentially for process control systems and has been used for petroleum, chemistry, and medical applications in China.

‡ Corresponding author

* Project supported by the National High-Tech R&D Program (863) of China (No. 2008AA042602) and the National Natural Science Foundation of China (Nos. 61075078 and 61074028)

According to IEC61784 (IEC-61784-1:2007; IEC-61784-2:2007), two of the most important real-time performance indicators are (1) delivery time and communication cycles and (2) the number of end nodes. Delivery time means the total latency to convey a data frame from one node to another. It is measured at the application layer. The communication cycle is a time period during which the communication is repeated. In an EPA scenario, the delivery time is around several milliseconds and the communication cycle is generally more than 10 ms. End nodes are used for transmitting input and output data in the network. The output data is usually generated for the actuators and the input data for the sensors. The number of end nodes in an EPA network varies from a few to several hundred.

Control systems have been more and more intelligent and flexible, and thus need faster communication systems with higher real-time requirements. These systems can be called fast real-time (FRT) systems or synchronization systems (Sauter, 2007). A large scale inverter control system, for example, requires a communication cycle of several milliseconds and hundreds of end nodes (Raja *et al.*, 1994). The current EPA protocol has to be improved to satisfy these requirements.

Although there is not a precise definition of an FRT system, we can generally consider that in an FRT system, the communication cycle is required to be less than 1 ms and the delivery time jitter no more than 1 μs (Felser, 2005). The most severe case is when a large amount of small periodic data needs to be transmitted in a very short time interval.

Given the communication cycle and network bandwidth, to increase the number of end nodes as much as possible, the bandwidth utilization should be as high as possible. However, a small cyclic payload may bring about a great amount of redundant data and protocol overhead due to the minimum frame length in Ethernet. This is a big obstacle to increasing bandwidth utilization.

An FRT strategy in the EtherCAT protocol proposed by Beckhoff introduced a modified Ethernet physical layer to deal with the FRT systems (Prytz, 2008; Vitturi *et al*., 2011). The physical network interfaces had been redesigned to allow the extraction/insertion of information from/to a frame when it is passing through a node. These modifications could make the communication cycle down to 300 μs and bandwidth utilization up to 90%. However, EtherCAT needs substantial modifications in low layers of the network and has shortcomings for large cyclic payload (Jasperneite *et al*., 2007; Gaderer *et al*., 2010; Cena *et al*., 2012). The FRT (also named isochronous real-time, IRT) strategy in PROFINET/IRT also needs major modifications in low layer interfaces, which may lead to incompatibility with the original Ethernet (Ferrari *et al*., 2006; Schumacher *et al*., 2008; Gao *et al*., 2010). The nodes in an FRT system must be redesigned, and fast hardware structure such as field-programmable gate array (FPGA) or digital signal processor (DSP) must be used (Cereia *et al*., 2011; Monmasson *et al*., 2011; Kim *et al*., 2012). Ethernet Powerlink can also be adopted in FRT scenarios by some modifications (Hanzalek *et al*., 2010). There are also studies on RTE for motion control or fast computer numerical control (CNC) systems where certain protocol modifications or special scheduling schemes are added to the protocol to improve the real-time performance (Ferrari *et al*., 2010; Erwinski *et al*., 2013). Besides, synchronization accuracy is required to be improved in all FRT applications (Chen and An, 2010; van den Heuvel *et al*., 2012).

The idea of this work is a new FRT scheme based on an EPA network, which keeps the EPA-FRT based network backward compatible with the original EPA network at the physical level. To improve the real-time performance and achieve higher bandwidth utilization, the EPA frame format is simplified and the synchronization process is optimized to improve the accuracy. Most importantly, a multi-segmented scheduling scheme is developed to increase effective bandwidth utilization and reduce protocol overheads, and thus to shorten the communication cycle.

Beginning with a basic specification of the EPA protocol, we give a network model and study the time properties of the protocol in detail. The main problems the EPA protocol faces in FRT scenarios are outlined. An EPA-FRT scheme is proposed along with a multi-segmented scheduling algorithm. Finally, performance of the new EPA-FRT system with a multi-segmented structure is evaluated. Simulation and experimental results verify the effectiveness of the multi-segmented scheduling scheme, especially at small payload.

2 Ethernet for plant automation (EPA) protocol

2.1 Overview

To eliminate the network induced delay brought by CSMA/CD, a communication scheduling management entity (CSME) is introduced between the MAC layer and the data link layer of the Ethernet. CSME manages the communication process in time division multiple access (TDMA) mode to achieve real-time deterministic communications. To maintain compatibility with existing Ethernet based networks, the MAC and PHY (physical) layers defined in IEEE 802.3 are adopted without any change in the EPA network. Fig. 1 shows the whole protocol stack.

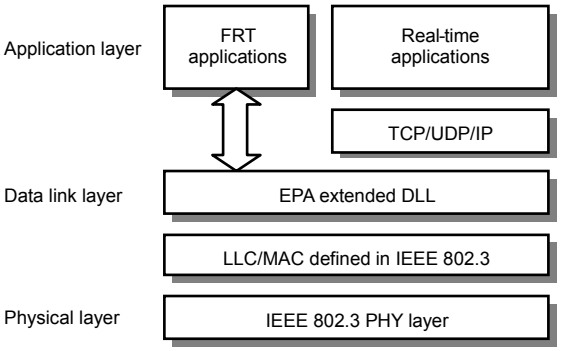

Fig. 1 EPA protocol stack structure

2.2 Communication process

Except that one dedicated node must be set as the master for clock synchronization, the EPA network works in a basic distribution mode. There is no specific station to manage the communication process and the status of each node is identical. The communication process is divided into equal cycles, defined as macrocycles (Fig. 2). Macrocycle is the basic communication interval. A macrocycle can be further divided into two phases, namely the periodic message transferring (PT) phase and the non-periodic message transferring (NT) phase, for the periodic and non-periodic messages, respectively.

In a certain PT phase, a node is allocated zero, one, or more independent time slots in which the node can emit its own periodic messages. Each time slot is set according to an offset time using a predefined timetable. The local clock of each node must be synchronized so that each node can determine its own time offset to the beginning of every macrocycle.

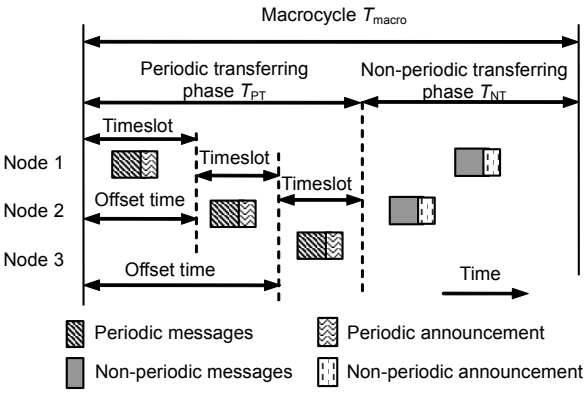

Fig. 2 Communication process in a macrocycle

Although the timetable in a PT phase is not prescribed by the EPA protocol, there is no mandatory provision that each node must be assigned one time slot in a same macrocycle. To deal with the periodic messages generated at various rates, the timetable can be changed according to different macrocycles. A scheduling algorithm and a bandwidth allocation scheme can be adopted in the PT phase.

In the NT phase the messages are transmitted according to their priorities. The time-critical messages like alarms and notifications have the highest priority and are transmitted first in the NT phase. The time-available messages like programs, download data, configuration files, and video streams have a relatively low priority and must be transmitted after all the time-critical messages have been sent out in the NT phase.

Distributed priority scheduling is based on two types of frame, periodic announcement and non-periodic announcement. Periodic announcements are broadcasted by each node after the node has just sent its periodic messages to inform the other nodes of the priority of its non-periodic messages. Non-periodic announcements are broadcasted by each node after the node has just sent its non-periodic messages to inform the other nodes of its finishing the transmission, so that other nodes can continue their transmissions. Each node in the NT phase needs to listen to the broadcasted non-periodic announcement to trigger the transmission.

The frame format of EPA is compatible with an Ethernet frame. The MAC, Internet Protocol (IP), and User Data Protocol (UDP) heads are adopted without modifications.

2.3 Topology

The topology in EPA networks is not restricted in the protocol. Any basic structure, such as tree, line, or a combination thereof, can be seen as a single bus structure in that only one node is allowed to send the message at a time. Switches and/or hubs can be used to link the nodes in EPA networks. According to the working mechanism of the CSMA entity, a full-duplex mode is not mandatory, and a hub-based architecture is still feasible in EPA networks.

Common switches can be used directly in EPA networks. They are not recommended, however, as they will bring about extra latencies to the store and forward process of the switch.

As a matter of fact, a segmented network would be a better topology in applications where there are several independent services in the network. As single bus structure is the most representative topology in EPA, the single-bus condition is assumed for the analysis of the performance of the EPA protocol.

2.4 Clock synchronization

EPA uses the IEC 1588 Precise Time Protocol (PTP) (IEEE1588:2008) for clock synchronization. All the nodes in the network are synchronized to the master clock node.

There are four kinds of frames for synchronization service: Sync, Follow_up, Delay_Req, and Delay_Resp (Fig. 3). In a node-to-node synchronization process, the master clock node is called the master and the other nodes the slaves.

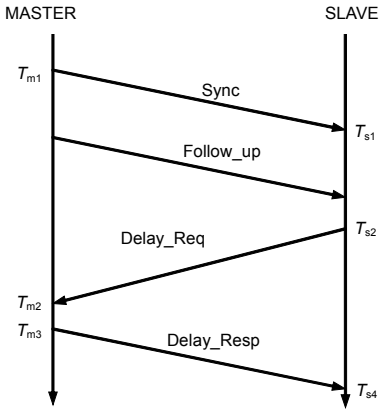

Fig. 3 Time stamp in the synchronization process

There are two phases in the synchronization process. One is the sync phase in which a pair of Sync and Follow_up frames is transmitted between the master and the slave to inform the slave of the offset time. The other is the Req-Res phase in which a pair of Delay_Req and Delay_Resp frames is transmitted for the calculation of the line delay between the master and the slave.

The line delay is calculated by

$$\text{Line\_delay}=[(T_{m2}-T_{m1})-(T_{s2}-T_{s1})]/2. \quad (1)$$

The offset time of the slave to the master is calculated by

$$\text{Offset}=T_{s4}-(T_{m3}+\text{Line\_delay}). \quad (2)$$

T_{m1}, T_{m2}, T_{m3}, T_{s1}, T_{s2}, T_{s4} are the time stamps in the synchronization process (Fig. 3).

The accuracy of clock synchronization is determined by the synchronization error, which is the maximum absolute value of the offset times of the slave clocks to the master clock in the whole network.

The synchronization error comes from two sources. One is the oscillator deviation among the master clock node and the slave clock nodes. Even if all the nodes are perfectly synchronized by a Sync frame at one moment, the synchronization error may increase due to oscillator deviation. The other is the calculation error of the line delay, which may lead to an erroneous offset time.

In the EPA protocol, synchronization frames are transmitted in the NT phase and have the highest priority. If network topology is stable, the line delay will not change much during the operation of the system. Then the main influencing factor of the synchronization error is the oscillator deviation in EPA nodes. As oscillator deviation cannot be easily eliminated, increasing the frequency of sending the Sync and Follow_up pair is an effective way to improve synchronization accuracy.

2.5 Timing analysis

As EPA is designed originally for process control applications in which real-time constraints are not critical, there will be some timing problems if it is adopted in FRT control networks without proper modifications. To outline these problems, we present a thorough analysis of the time properties of EPA networks, including the relationships among different time slot durations, synchronization errors, node number, and data lengths.

Some parameters are defined as follows: T_{macro}, duration of a macrocycle; T_{PT}, duration of a periodic phase; T_{NP}, duration of a non-periodic phase; B, network bandwidth; N, number of nodes in the system, including one main controller and $N-1$ input/output nodes; T_{syn}, synchronization error; L_p, L_{np}, L_{pa}, L_{npa}, the frame lengths of a periodic frame, a non-periodic frame, a periodic announcement, and a non-periodic announcement respectively, each including the preamble code, frame gap, and cyclic redundancy check (CRC) fields; P, payload data length of a periodic frame.

To obtain the theoretical lower bound of the macrocycle and upper bound of bandwidth utilization, we make seven assumptions for timing analysis. Some of the assumptions do not accord with practical applications, but they are helpful in finding the shortcomings of the EPA protocol.

Assumption 1 All the nodes work in time-trigger mode.

Assumption 2 No retransmission mechanism is used and the corrupted frame is discarded.

Although there is a necessity to adopt a retransmission scheme to correct the errors in the transmission process, this assumption is made for two reasons. One is that the error rate can be significantly reduced by using high reliable PHY interfaces. The other is that the retransmission for a corrupted frame will be invalid in an FRT system because of the high data update rate. Even if the corrected frame is received through a retransmission process, the data will be out of date for the control process; thus, we usually discard the corrupted frame by a CRC. Or we can consider that the transmission error is neglected in this analysis, as in Decotignie (2005).

Assumption 3 All delays due to hardware/software implementation in the sending/receiving/forwarding processes are summarized as the implementation delay, constant and proportional to the frame length.

Let d be the implementation delay parameter. The implementation delay can be expressed as dL, where L is the frame length.

The implementation delay can be reduced by the optimization of hardware/software implementations and also the network structure. In an ideal condition, d=0.

Assumption 4 The payloads in all periodic frames are the same.

In fact, there could be a multitude of periodic services in a control system to monitor different variables with different payload sizes. This assumption is used to make clear the relationship between the periodic payload size and the minimum macrocycle in our study.

Assumption 5 All periodic frames are generated in a same cycle, which is the macrocycle.

The practical situation may be different from this assumption. A scheduling scheme in Hong and Song (2008) can be used to cope with periodic frames generated at various rates. The idea is to let two or more nodes share one timeslot. This assumption is made to simplify the time slot configuration for timing analysis. The EPA protocol can handle periodic frames generated at various rates in actual applications.

Assumption 6 The system works in a general case.

Although the communication relationships among the nodes may be complicated and vary with different applications, we assume a general case in which there is only one main controller node in the network. In every macrocycle, the main controller sends one periodic frame (output data) to all the other nodes and receives one periodic frame from each of them (input data). There may also be data exchange among nodes other than the main controller node in some applications. However, the data exchange will be handled through the main controller node and there is no direct data exchange among those nodes.

Assumption 7 Communications in the NT phase are more complicated than in the PT phase.

Here we consider a very conservative case where all nodes send a very urgent frame that must be transmitted in the current NT phase.

2.6 EPA timing

A TDMA based timeslot allocation scheme is the kernel in the EPA communication process. According to Fig. 2, the duration of a macrocycle can be expressed as

$$T_{macro}=T_{PT}+T_{NT}. \tag{3}$$

As shown in Fig. 2, the duration of a PT phase is determined by the duration of timeslots:

$$T_{PT}=\sum_{i=1}^{N}T_{slot}^{i}, \tag{4}$$

where T^i_{slot} is the timeslot duration of the ith node. Assume timeslot T^1_{slot} is assigned to the main controller. The duration of a timeslot can be further expressed as

$$T^i_{\text{slot}}=\begin{cases}(L_{\text{p}}+L_{\text{pa}})(1/B+d)+T^i_{\text{idle}}, & i\neq 1,\\ [(N-1)L_{\text{p}}+L_{\text{pa}}](1/B+d)+T^i_{\text{idle}}, & i=1,\end{cases} \tag{5}$$

where T^i_{idle} is the sum of idle times reserved at the beginning and the end of the timeslot of the ith node (Fig. 4).

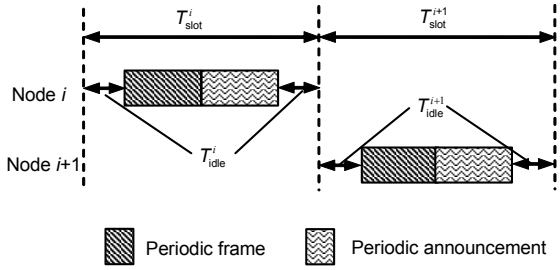

Fig. 4 Timing in a timeslot

The timeslots in EPA are set according to the prescribed offset times. In the ideal situation, all the nodes are perfectly synchronized so that the offset times should be the prescribed values exactly. However, the actual offset time will deviate from the setting value due to the synchronization error.

If the reserved idle time is not long enough, there will be a collision between a periodic announcement and a periodic frame (Fig. 5).

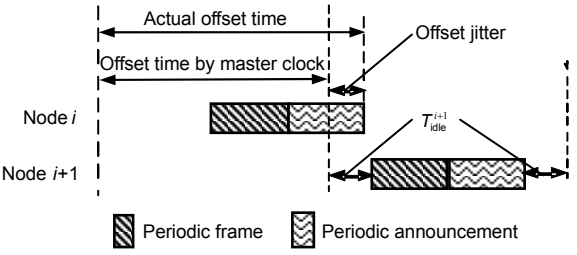

Fig. 5 Offset jitter in a timeslot

To guarantee that no collision occurs, the minimum idle time will be set to

$$T_{\text{idle}}=2T_{\text{syn}}. \tag{6}$$

According to Eqs. (4)–(6) the duration of the PT phase can be expressed as

$$T_{\text{PT}}=\sum_{i=1}^{N}T^i_{\text{slot}}=[(2N-2)L_{\text{p}}+NL_{\text{pa}}](1/B+d)+2NT_{\text{syn}}. \tag{7}$$

In the NT phase, a node must receive the previous frame before it can decide whether it is its turn to send the frame. This will lead to a hardware delay in detecting the announcement and make a time gap between two non-periodic frames along the NT communication process. Let L_{idle} be the extra equivalent frame length of the time gap. According to Assumption 7, the duration of the NT phase can be expressed as

$$\begin{aligned}T_{\text{NP}}&=\sum_{i=1}^{N}(L_{\text{np}}+L_{\text{npa}}+L_{\text{idle}})(1/B+d)\\ &=N(L_{\text{np}}+L_{\text{npa}}+L_{\text{idle}})/(1/B+d).\end{aligned} \tag{8}$$

The minimum duration of the macrocycle is

$$\begin{aligned}\min(T_{\text{macro}})=&(2N-2)L_{\text{p}}(1/B+d)\\ &+NL_{\text{pa}}(1/B+d)+2NT_{\text{syn}}\\ &+N(L_{\text{np}}+L_{\text{npa}}+L_{\text{idle}})(1/B+d).\end{aligned} \tag{9}$$

In a practical case, the duration of the NT phase depends on the generation rate of the non-periodic messages. As a result, we focus mainly on the timing properties and the real-time metrics in the PT phase.

A complete periodic frame is composed of data payload, protocol overhead, and redundant padding. Payload is the useful data that needs to be transmitted. Protocol overhead contains the necessary communication information in the EPA protocol. Redundant padding has no actual meaning except that it makes a frame up to the required length be transmitted in the Ethernet. The frame length is thus the sum of the lengths of data payload, protocol overhead, and redundant padding. Eq. (9) turns into

$$\begin{aligned}\min(T_{\text{macro}})=&(2N-2)(P+O+R)(1/B+d)\\ &+NL_{\text{pa}}(1/B+d)+2NT_{\text{syn}}\\ &+N(L_{\text{np}}+L_{\text{npa}}+L_{\text{idle}})(1/B+d),\end{aligned} \tag{10}$$

where O is the total length of the protocol overhead in

a periodic frame, and R is the length of redundant padding in a periodic frame. If the total length of protocol overhead and payload is less than the minimum length of an Ethernet frame, redundant padding needs to be added. Here the minimum Ethernet length is 84 bytes, including the frame gap and preamble code.

To analyze the payload transmitted in a macrocycle, especially in the PT phase, a conception of 'effective bandwidth utilization' is introduced.

Definition 1 (Effective bandwidth utilization, U_e) Effective bandwidth utilization is the ratio of the total payload transmitted in the network to the maximum traffic that can be transmitted in the network in a time interval t:

$$U_e = \sum \text{Payload} / (tB), \tag{11}$$

where $\sum \text{Payload}$ is the sum of the payloads transmitted in a long time interval t.

Then the effective bandwidth utilization in the PT phase is

$$U_e = \sum P / (T_{PT} B) = \frac{(2N-2)P}{[(2N-2)L_p + NL_{pa}](1+dB) + 2NT_{syn}B}. \tag{12}$$

2.7 Problems in EPA

The minimum macrocycle is an important performance indicator of real-time industrial networks. A shorter macrocycle means a higher system sampling rate. Meanwhile, if the minimum macrocycle is smaller than the sampling cycle that the system requires, more nodes can be added to the network.

In an ideal condition, d=0. According to Eq. (12), given the node number N and the payload P, the maximum effective bandwidth utilization determines the minimum duration of the PT phase.

In the EPA protocol, the protocol overhead in Eq. (12) is 68 bytes including 8 bytes of preamble code, 12 bytes of frame gap, 4 bytes of CRC, and 44 bytes of EPA head. The length of the periodic announcement is 84 bytes.

In FRT scenarios the periodic payload is several bytes in most cases. Here we take 4 bytes as an example. Even when the clocks are perfectly synchronized (T_{syn}=0), the effective bandwidth utilization is 3.1% when N=10 and 3.2% when N=100, according to Eq. (12). Considering that the synchronization error is around 10 μs or more in process control systems, the practical effective bandwidth utilization may be under 3%. An extremely low effective bandwidth utilization makes it difficult to minimize the macrocycle.

The analysis of effective bandwidth utilization provides clues to improving the real-time performance of EPA networks. Since we cannot easily reduce the payload, the only way to minimize the macrocycle is to increase the effective bandwidth utilization. Based on Eq. (12), feasible improvements are: (1) reducing the protocol overhead O and the redundant padding R; (2) increasing the synchronization accuracy to reduce the synchronization error T_{syn}; (3) increasing the payload in a single frame to decrease the frame number in the backbone network bus.

3 EPA-FRT scheme

3.1 Reducing the protocol overheads

First, the EPA header is redesigned to remove the useless data in the IP header and UDP header. Only indispensable information fields are reserved.

To increase synchronization accuracy, the frequency of Sync and Follow_up should be increased, and thus the synchronization service will occupy a considerable bandwidth, which is inefficient in an FRT system.

Second, the information fields in Sync and Follow_up frames are integrated into the EPA header in the periodic frames to reduce synchronization overhead. However, the Follow_up information cannot be obtained until the frame is sent out. As a result, the Sync and Follow_up frames appear in pairs (Fig. 6). The Follow_up information in one periodic frame refers to the frame in the previous macrocycle. As the macrocycle is very short in FRT systems, this modification can also increase the frequency of sending Sync and Follow_up frame pairs, resulting in an improvement of synchronization accuracy.

Third, the information fields in a periodic announcement are integrated into the periodic frame and those in a non-periodic announcement into the non-periodic frame. Fig. 7 illustrates the frame format of a periodic frame.

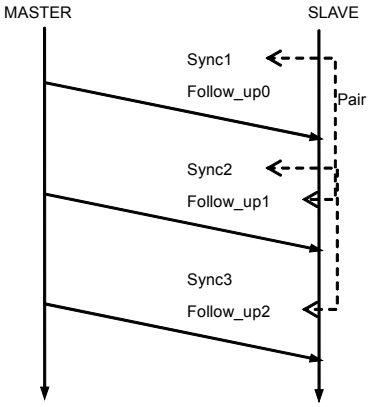

Fig. 6 Synchronization process in the fast real-time (FRT) scheme

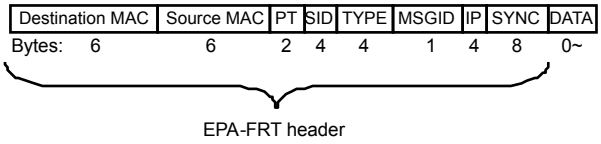

PT: protocol type (0x88CB); SID: service ID; TYPE: frame type; MSGID: sequence ID to select the redundant route; IP: IP address; SYNC: clock synchronization information

Fig. 7 Frame structure in the fast real-time (FRT) scheme

3.2 Multi-segmented structure

Traditional network segmentation is a technique to enforce parallelization of flows if the flows are independent of each other. The new segmentation scheme in this work, however, is to cope with a single flow of data.

To reduce the redundant padding, the payload should be increased in each single periodic frame. The very idea of our multi-segmented scheduling scheme is to divide the whole network into several parallel subnets named segments in which the data in a frame can be distributed and aggregated.

For the input data, the periodic frames in one segment are sent to one certain node. The payload is extracted from these periodic frames and then aggregated into a new periodic frame. The payload in the new periodic frame will be increased to eliminate the redundant padding. In the meantime, the number of periodic frames is decreased with reduction of aggregation and protocol overhead.

For the output data, a broadcast mechanism is used. The periodic payload from the main controller is integrated into one periodic frame (if the data length exceeds the maximum Ethernet length, two or more such frames will be used) and then broadcasted to other nodes. Each node will fetch only its own periodic data from the broadcasted frame.

First we define the concepts of 'segment' and 'relaying node' in EPA-FRT.

Definition 2 (Segment) A network segment is a collision domain in which a collision will occur if a frame is sent to the network bus before the previous frame has been completely transmitted.

Definition 3 (Relaying node) A relaying node is a node connected to two segments. The relaying nodes aggregate and distribute data in the network. In general, there are three kinds of nodes in the multi-segmented network: main controller node, relaying nodes, and normal nodes.

A multi-segmented network consists of a backbone network and branch segments. The backbone network is the segment to which the main controller is connected. It contains only the main controller and relaying nodes. The branch segments are the other segments under the backbone network. A branch network contains normal nodes and only one relaying node. The network topologies in the backbone or the segment networks are not specified in the multi-segmented scheme. They can be of any type, such as line, tree, or ring structure. In this work, we use bus structure as the example.

The multi-segmented structure can be any topology with a multi-level and multi-way tree structure. However, the network structure of three or more levels may be complicated, leading to significant increase in the forward delay. Two-level structure is a better choice and we will focus on this structure in this work.

Fig. 8 shows a typical example of the two-level multi-segmented network with a line structure. There are mn+1 nodes including the main controller in the network. The nodes are arranged in a matrix with m rows and n columns. The first column of the matrix is the backbone network and each row of the matrix is a segment.

Matrix structure is not the only possible structure in the multi-segmented scheme. There are other dividing methods such as three or more levels structuring, segmenting according to physical placement, or averaging data load among the segments. Here we choose matrix structure as a typical example, which proves effective in performance analysis of EPA-FRT networks in the following.

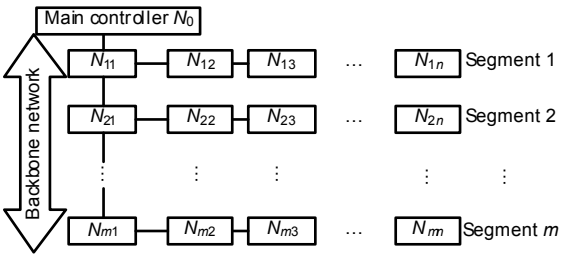

Fig. 8 Multi-segmented structure in the fast real-time (FRT) scheme

The total number of nodes in the network is

$$N=mn+1. \tag{13}$$

When $N-1$ cannot be expressed as product of two integers greater than 1, the number of nodes in the last segment (last row) will be smaller than that in any other segment. Then we have

$$N=n(m-1)+k+1,\ 0\le k\le n, \tag{14}$$

where k is the node number in the last segment.

3.3 Multi-segmented timing

Assumption 6 is used in this subsection for a better illustration.

Once the network has been divided into separate segments, the periodic frames in different segments can be transmitted simultaneously. A new communication timetable (Fig. 9) is required in the multi-segmented structure to enable parallel communications in different segments.

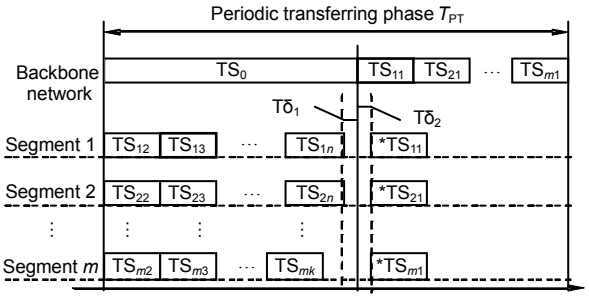

Fig. 9 Multi-segmented timetable in the periodic transferring phase

The PT phase can be divided into two parts, distribution and aggregation. First, the main controller sends the periodic frames to the relaying nodes in a large aggregated frame (if a frame of 1538 bytes is not enough to contain all the data, two or more frames will be used). This frame contains all the output payloads to the nodes in the network. At the same time, normal nodes send their periodic frames to the relaying nodes in a TDMA sequence as in the original EPA protocol. Afterwards, each relaying node aggregates the payload from its segment and sends it to the main controller in one or more large aggregated frames. In the meantime, each relaying node extracts the periodic data from the main controller and then distributes the periodic data by newly generated frames to the normal nodes in its segment. Thus, each relaying node is allocated two timeslots, one for the backbone network and the other for its branch segment.

The timeslot of node N_{ij} is expressed as TS_{ij}. The timeslots of the relaying nodes in the backbone network and branch segment are expressed as TS_{ij} and $*TS_{ij}$, respectively. The duration of the first part in the PT phase is determined by the maximum of TS_0 and $\sum_{j=2}^{n} TS_{ij}$ (i=1, 2, …, m), and the duration of the second part in the PT phase is determined by $\sum_{i=2}^{m} TS_{i1}$.

$T\delta_1$ and $T\delta_2$ are defined as the reserved time durations for frame aggregation and frame distribution in the relaying nodes, respectively. In fact, if the aggregation and distribution are achieved by an FPGA or application specific integrated circuit (ASIC) based hardware, there will be little processing delay during the aggregation and distribution processes. These delays can be reduced to several nanoseconds and neglected compared to the duration of a timeslot. Thus, $T\delta_1$ and $T\delta_2$ are not included in the timing analysis.

The duration of TS_0 is

$$\begin{aligned} TS_0 &= [(N-1)P+O](1/B+d)+2T_{\text{syn}} \\ &\quad +\lfloor (N-1)P/1479 \rfloor O(1/B+d), \end{aligned} \tag{15}$$

where 1479 bytes is the maximum payload length in a periodic frame. If the payload exceeds the maximum length, two or more periodic frames are used. Thus, the extra protocol overhead $\lfloor (N-1)P/1479 \rfloor O/B$ is included.

The duration of TS_{i1} is

$$TS_{i1} = (nP + O)(1/B + d) + 2T_{syn} + \lfloor nP/1479 \rfloor O(1/B + d). \tag{16}$$

The duration of $*TS_{i1}$ is

$$\begin{aligned} *TS_{i1} &= [(n-1)P + O](1/B + d) + 2T_{syn} \\ &\quad + \lfloor (n-1)P/1479 \rfloor O(1/B + d). \end{aligned} \tag{17}$$

The duration of the PT phase is

$$T_{PT} = \max\left(TS_0, \sum_{j=2}^{n} TS_{1j} \right) + \sum_{i=1}^{m} TS_{i1}. \tag{18}$$

Given N and P, to reach the minimum PT phase, we need to find the optimized value of m. As the node number is a constant, the duration of TS_0 depends only on the payload and cannot be reduced. So, the minimum duration of the first part of the PT phase is at least the duration of TS_0. To achieve a minimum PT phase, the second part of the PT phase should be as short as possible, which means m should be as small as possible. Also, n should be small enough to guarantee that

$$\sum_{j=2}^{n} TS_{ij} \le TS_0, \quad i=1, 2, \ldots, m.$$

Then we have

$$\begin{aligned} \sum_{j=2}^{n} TS_{1j} &= (n-1)(P + O + R)(1/B + d) + 2(n-1)T_{syn} \\ &\le (NP - P + O)(1/B + d) + 2T_{syn} \\ &\quad + \lfloor (N-1)P/1479 \rfloor O(1/B + d). \end{aligned} \tag{19}$$

The duration of the PT phase is changed to

$$\begin{aligned} T_{PT} &= TS_0 + \sum_{i=1}^{m} TS_{i1} \\ &= [(N-1)P + O]/B + 2T_{syn} + 2mT_{syn} \\ &\quad + \lfloor (N-1)P/1479 \rfloor O(1/B + d) \\ &\quad + [(N-1)P + Om](1/B + d) \\ &\quad + (m-1)\lfloor nP/1479 \rfloor O(1/B + d) \\ &\quad + \lfloor kP/1479 \rfloor O(1/B + d). \end{aligned} \tag{20}$$

The PT phase reaches the minimum duration while

$$\begin{aligned} m = \lceil (N-1)[(P + O + R)(1/B + d) + 2T_{syn}] \\ \cdot [(NP + 2O + R)(1/B + d) \\ + \lfloor (N-1)P/1479 \rfloor O(1/B + d) + 4T_{syn}]^{-1} \rceil. \end{aligned} \tag{21}$$

The non-periodic frames are still transmitted on a priority basis. The relaying nodes work just like a switch.

In the worst case the duration of the NT phase is

$$T_{NT} = (N + L_{idle})L_{np}(1/B + d). \tag{22}$$

The minimum macrocycle is

$$\min(T_{macro}) = \min(T_{PT}) + T_{NT}. \tag{23}$$

To calculate the transmission delays of the periodic and non-periodic frames, a very conservative case is considered. If a periodic frame is generated at the beginning of the NT phase, it would take at most a whole macrocycle to transmit the periodic frame. If a non-periodic frame is generated at the beginning of the PT phase, the transmission time in the worst case is still a macrocycle.

A multi-segmented network is set up as follows:

Given: node number N, payload length P, maximum allowable delays of periodic and non-periodic frames D_p and D_{np}.

Step 1: Estimate the synchronization error T_{syn}.

Step 2: Calculate TS_0 according to Eq. (15) and minimum segment number m according to Eq. (21).

Step 3: Calculate the duration of the macrocycle according to Eq. (23). Build the multi-segmented network and test the synchronization error $*T_{syn}$ with the macrocycle obtained from Eq. (23).

If ($*T_{syn} > T_{syn}$) (meaning that the synchronization error is underestimated)

Set $T_{syn} = *T_{syn}$ and go to step 1;

Else If ($T_{macro} > D_p$) or ($T_{macro} > D_{np}$) (meaning that the delay requirement is not satisfied)

Reduce the node number or the payload length and go to step 1;

Else

The configuration is completed.

4 Performance evaluation

To prove the effectiveness of the EPA-FRT scheme and find out under which situation the EPA-FRT network will achieve the best performance, we evaluate the new EPA-FRT network by both theoretical analysis and experimental tests. The performance is evaluated by calculating the two most important indicators, the minimum macrocycle and the effective bandwidth utilization, in an ideal condition where there are no hardware/software delays in the network and the implementation delay is set to zero.

A fast Ethernet with a bandwidth of 100 Mb/s is assumed. The NP phase is set to zero to achieve a minimum macrocycle and no non-periodic frame is transmitted in the network after the network configuration is completed.

According to the protocol profiles, the relevant parameters are listed in Table 1. T_{syn} and L_{idle} are obtained from the prototype system tests in the next section.

Table 1 Parameters of the EPA and EPA-FRT protocols

Parameter	Value	
	EPA	EPA-FRT
Total length of protocol overhead in a periodic frame, O (byte)	66	59
Network bandwidth, B (byte/s)	12.5×10^6	12.5×10^6
Synchronization error, T_{syn} (μs)	1.0	0.5
Length of redundant padding in a periodic frame, R	max(0, 18−P)	max(0, 25−P)
Frame length of a periodic announcement, L_{pa} (byte)	84	N
Extra equivalent frame length of the time gap, L_{idle} (byte)	11	11
Implementation delay, d	0	0

P: payload data length of a periodic frame; N: node number

First, the minimum macrocycles of EPA and EPA-FRT networks are given as a function of the number of nodes with different payloads of 2, 16, 128, and 512 bytes. The simulation results of the EPA network (Fig. 10a) show that the minimum macrocycle increases linearly with the increase of the number of nodes. For a specific number of nodes, the minimum macrocycle is identical when the payload is 2 or 16 bytes. The reason is that when the payload is no more than 22 bytes, a whole frame of 84 bytes is always needed to transmit the effective data, so the minimum macrocycle makes no difference. When the payload is more than 22 bytes, the minimum macrocycle increases with the increase of payload length.

The results in the EPA-FRT network in Fig. 10b, however, show a different trend. There is an obvious distinction between the minimum macrocycles when the payload is 2 or 16 bytes, owing to the frame aggregation mechanism. Besides, the payload has a greater influence on the minimum macrocycle.

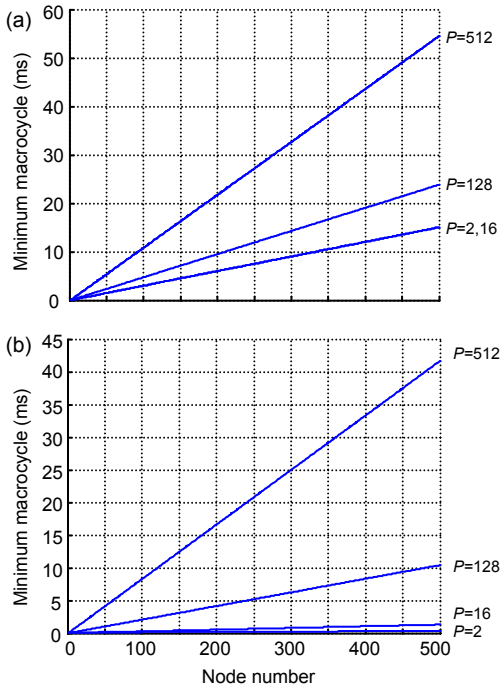

Fig. 10 Minimum macrocycle vs. the node number in EPA (a) and EPA-FRT (b) networks for different payload lengths

Next, the minimum macrocycle of the EPA or EPA-FRT network is given as a function of the payload with different node numbers of 5, 25, 100, and 500 (Fig. 11). Fig. 11a also shows that the minimum macrocycle in an EPA network depends mainly on the node number rather than the payload. Figs. 10b and 11b show that the node number and payload both have a linear relationship with the minimum macrocycle in the EPA-FRT network.

To compare the minimum macrocycle between EPA and EPA-FRT networks, the results of the macrocycle ratio, T_{EPA}/T_{FRT}, are shown in Figs. 12 and 13. The EPA-FRT network has a remarkable advantage over the EPA network at a small payload

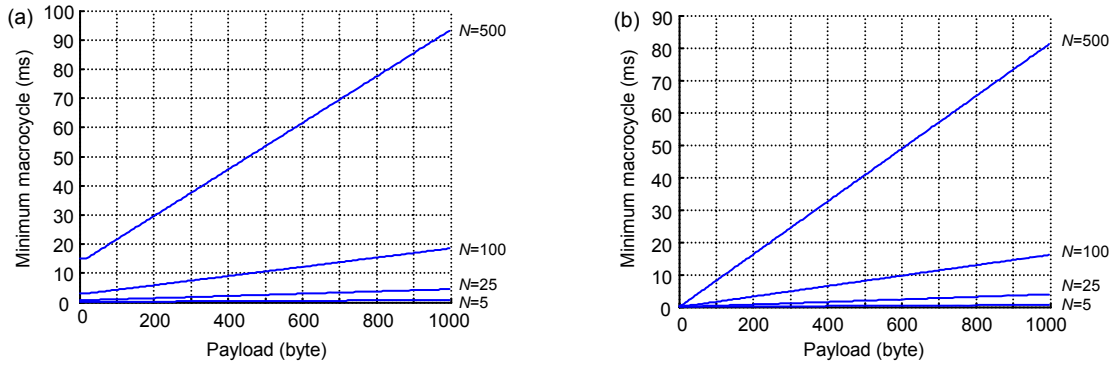

Fig. 11 Minimum macrocycle vs. payloads in EPA (a) and EPA-FRT (b) networks for different node numbers

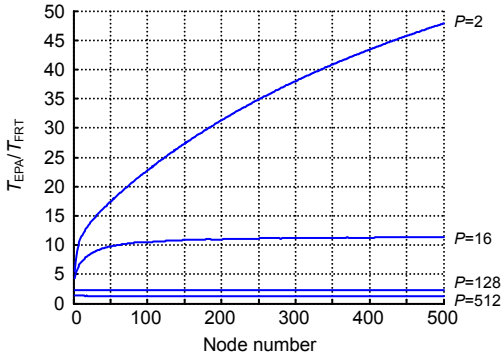

Fig. 12 The macrocycle ratio (T_{EPA}/T_{FRT}) vs. the node number for different payload lengths

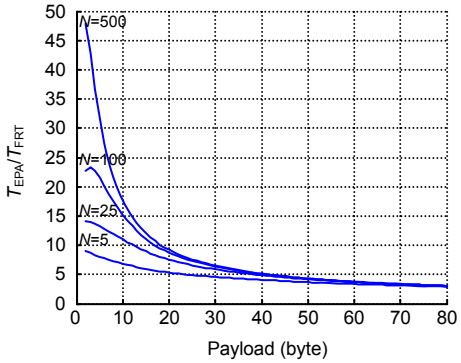

Fig. 13 The macrocycle ratio (T_{EPA}/T_{FRT}) vs. payload for different node numbers

and a large node number. The minimum macrocycle of an EPA-FRT network can be even less than 3% of the macrocycle in an EPA network with respect to a payload of several bytes. This advantage comes from the use of the multi-segmented scheme, which significantly reduces the overhead in the backbone network. On the other hand, T_{EPA}/T_{FRT} tends to be a fixed value when the payload is more than 60 bytes. In this case, the effect of the multi-segmented scheme is not obvious and the advantage comes mainly from the simplification of the frame format and the improvement of synchronization accuracy.

The results of effective bandwidth utilization in the two networks are shown in Figs. 14 and 15. In both networks, the effective bandwidth utilization depends mainly on the payload. In the EPA network, the effective bandwidth utilization is nearly independent of the node number. In contrast, in EPA-FRT networks, the effective bandwidth utilization increases with the increase of the node number. This reveals that the matrix network structure achieves a better performance at a large node number.

In EPA networks, due to announcement overhead and low synchronization accuracies, the effective bandwidth utilization is under 50%, and extremely low when the payload is 2 bytes. In contrast, in EPA-FRT networks the effective bandwidth utilization remains more than 90% in most cases. Even when the payload is 2 bytes, it reaches 50% when the node number is more than 500.

The above analysis shows that the EPA-FRT scheme is valid in various cases and extremely effective at small periodic payload and large system scale. In practical applications, however, software implementation and data aggregation/distribution may introduce extra delays in frame transmission.

5 Experimental results

A prototype system is set up to verify the performance of the EPA-FRT network. All the trials are conducted on a platform specified as follows: The normal FRT node is implemented based on an ARM7

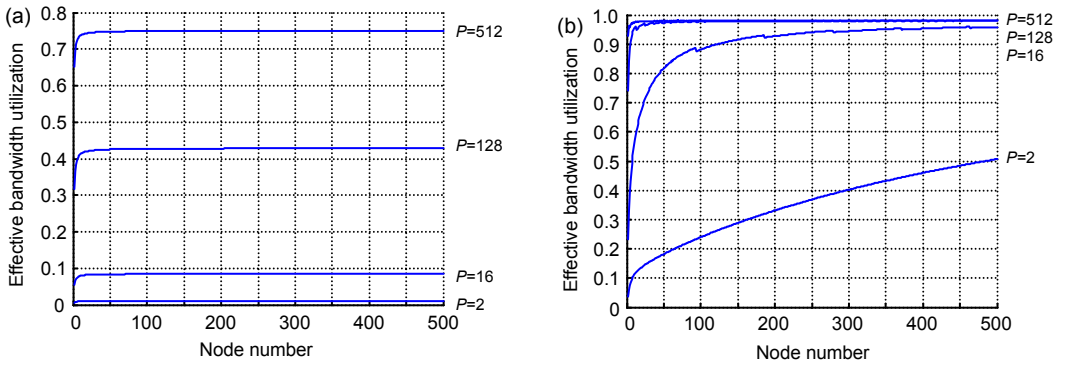

Fig. 14 Effective bandwidth vs. the node number in EPA (a) and EPA-FRT (b) networks for different payload lengths

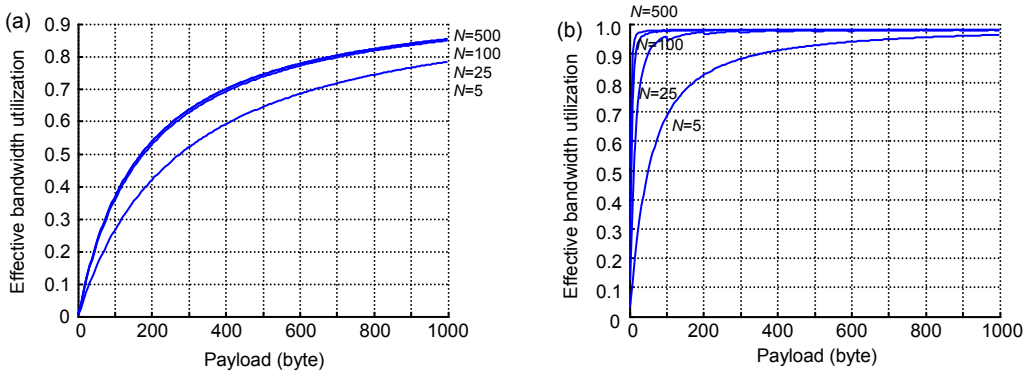

Fig. 15 Effective bandwidth vs. payload in EPA (a) and EPA-FRT (b) networks for different node numbers

processor (AT91R40008) with a clock frequency of 75 MHz. The Ethernet interface is implemented by a PHY chip with the MII interface (a 100 MB/s full-duplex mode is adopted). The two ports in one node forming the line structure are linked via a hub chip.

To reduce delays during the data aggregation and distribution processes, the relaying node is implemented by an FPGA architecture based on Cyclone II (EP2C20Q240C8) (Fig. 16). The two data flows of aggregation and distribution processes are separated, and their functions are implemented by individual modules, which will reduce the delay as much as possible.

All the FRT nodes are made as a sub-card which can be inserted in a main control board (Fig. 17). All the nodes are connected by specially designed high speed hubs to reduce the forwarding delay. One FRT sub-card is designated as the main controller and connected to the PC.

The test system is configured as a 4×4 matrix in a multi-segmented network mode with 4 relaying nodes and 12 normal nodes numbered as 0, 1, 2, …, 16. Among them nodes 1, 5, 9, 13 are relaying nodes and node 0 is the main controller (Fig. 18).

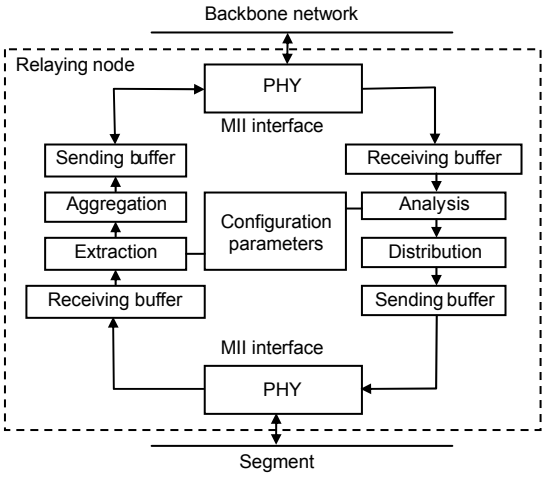

Fig. 16 Hardware structure of a relaying node

Each node sends one periodic frame to and receives one frame from the main controller in a macrocycle. All the periodic payloads are set to 2 bytes. To obtain the minimum macrocycle, the NT phase is set to a minimum duration which is just long enough to transmit a frame of 1538 bytes for the synchronization messages and configuration data. Fig. 19 shows the timeslot configuration of the system.

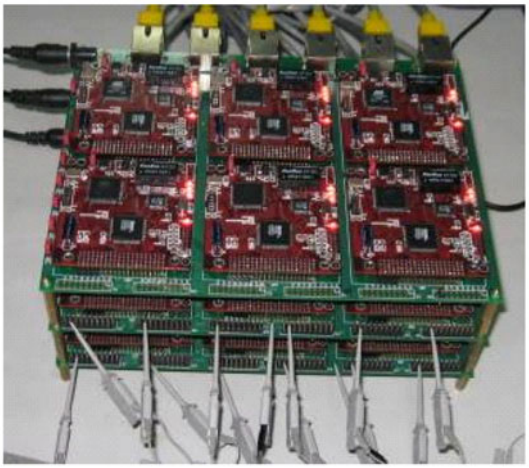

Fig. 17 Implementation of the prototype system

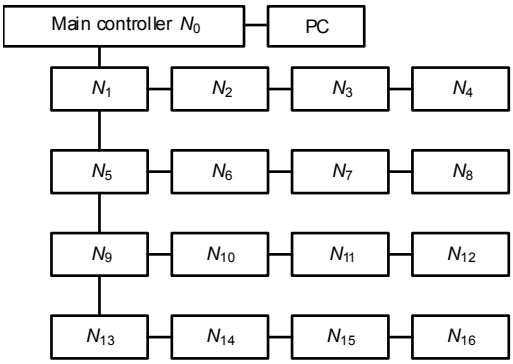

Fig. 18 Network structure of the test system

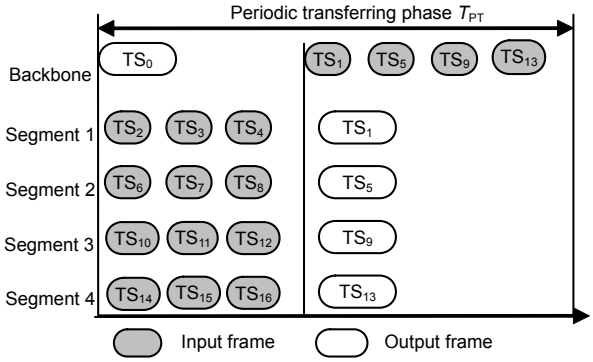

Fig. 19 Timeslot configuration in the EPA-FRT network

To obtain the local clocks of different nodes, a square-wave is output according to the clock counter inside each node. The rising edges of these square-waves are caught by the oscilloscope (Fig. 20).

In the minimum macrocycle test, the duration of the PT phase is first set to a relatively large value to be long enough for the transmission. Then we gradually adjust the offset time of each timeslot to reduce the macrocycle until we find the minimum time that still ensures a faultless transmission.

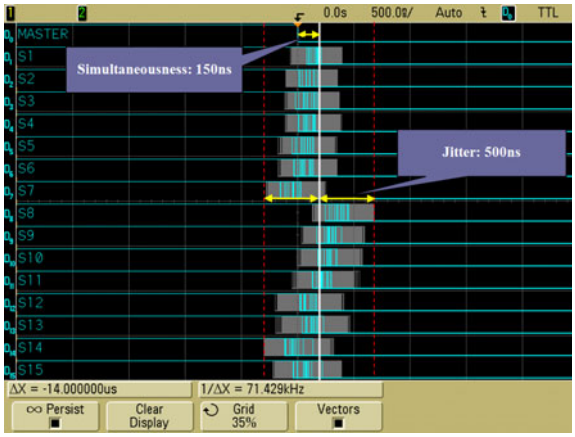

Fig. 20 Synchronization tests in the EPA-FRT network

Besides, another comparative system is implemented by the traditional EPA node based on an embedded design. Sixteen nodes are linked in a line structure and the periodic payloads are also set to 2 bytes. The rest are the same as the EPA-FRT experimental settings. All the transmission delays are measured in the application layer.

The test results are shown in Table 2.

Table 2 Test results from EPA and EPA-FRT networks

Parameter	Value	
	EPA	EPA-FRT
Synchronization error, T_{syn} (μs)	10	0.5
Minimum macrocycle (μs)	4346.40	279.33
Theoretical macrocycle (μs)	4254.30	265.64
Ideal minimum macrocycle (μs)	1253.76	179.96
Maximum transmission delay (μs)	134.02	267.23
Maximum transmission delay jitter (μs)	21.54	2.07

In the EPA network the Sync and Follow_up frame pair is broadcasted every second. As the frequency of transmitting the Sync and Follow_up frame pair has been notably increased in the EPA-FRT network, the synchronization error reduces from 10 μs to 500 ns.

The ideal minimum macrocycle is calculated when the implementation delays are neglected, and the implementation delay parameter, d, is field tested in both networks.

The tested macrocycles are larger than the ideal ones due to the implementation delays. EPA nodes are implemented on a software based embedded system. Software delay leads to considerable differences between the test results and the ideal ones in the EPA network. This difference can also be noted through the larger d in the EPA network (In fact, the EPA device is generally designed for the process industry where the macrocycle is set to around hundreds of milliseconds; thus, the requirement of the implementation delay is not so strict for the EPA node). In contrast, the implementation delay has been significantly reduced in the EPA-FRT network by a redesign of the nodes. The differences between the test results and the ideal ones are not remarkable because of a much smaller d.

The EPA-FRT system achieves much better performance than the EPA network and the macrocycle of the EPA-FRT network has been significantly reduced to less than 1 ms. Considering that there are only 16 end nodes in the network, the decrease of the minimum macrocycle of the EPA-FRT network will be more notable for a larger node number.

Note that the transmission delay jitter has been reduced in the EPA-FRT network, but contrary to what one might suppose, the maximum transmission delay has been increased due to the data aggregation process of the multi-segmented scheme. This can be seen from the timeslot configuration table in Fig. 19. The worst case occurs in the input frame of node 14. In fact, the multi-segmented scheme can ensure only that the maximum transmission delay does not exceed the PT time. This drawback should be allowed in the network configuration process. If the transmission delays are required to be within a very short interval, the multi-segmented approach should not be adopted.

From both theoretical calculations and actual tests, it can be concluded that the EPA-FRT scheme with the multi-segmented structure has improved the real-time performance of the EPA protocol. The EPA-FRT scheme shows its superiority especially for a small periodic payload and a short macrocycle. The EPA-FRT network cannot replace the EPA network, however, due to the increased hardware costs when adopting a more complex network topology. The EPA-FRT network would be much more appropriate for such scenarios as large scale inverter array control systems and motion control of humanoid robots, where the control cycle is relatively short, the periodic services and link relationships are relatively simple, and the frame payload is relatively small. The original EPA protocol, however, behaves better in process control systems or industrial video systems.

As the tests have not achieved ideal results, the EPA-FRT node performance of the prototype system can be further improved. For example, the node can be implemented by a fully integrated ASIC chip or a system-on-chip (SOC) platform; the implementation delays can thus be further reduced.

6 Conclusions

In this paper we propose an EPA-FRT scheme to improve the real-time performance and achieve higher bandwidth utilization. Analysis of the EPA protocol reveals that the synchronization accuracy and effective bandwidth utilization are the essential factors influencing the real-time performance. So, in the FRT scheme, the EPA frame format is simplified and the synchronization process is optimized to improve the accuracy. A multi-segmented scheduling scheme is presented to increase the effective bandwidth utilization and reduce the redundant protocol overhead, and thus to shorten the macrocycle.

Theoretical calculations and tests of a prototype system have proved the effectiveness of the EPA-FRT scheme. The simplified frame structure reduces the redundant overhead. The multi-segmented scheme significantly improves the effective bandwidth utilization in the backbone network, especially at a small periodic payload.

Due to delays introduced by software, the multi-segmented scheme leads to increase in transmission delays. These issues will be dealt with in future studies by, for example, optimizing the embedded system based cards with special EPA-FRT protocol chips to reduce software delay. As for the retransmission model, multi-segmented structures of three or more levels will be considered, and the timing model can be refined by incorporating a detailed delay analysis.

References

Cena, G., Bertolotti, I.C., Scanzio, S., Valenzano, A., Zunino, C., 2012. Evaluation of EtherCAT distributed clock performance. *IEEE Trans. Ind. Inf.*, **8**(1):20-29. [doi:10.1109/TII.2011.2172434]

Cereia, M., Bertolotti, I.C., Scanzio, S., 2011. Performance of a real-time EtherCAT master under Linux. *IEEE Trans. Ind. Inf.*, **7**(4):679-687. [doi:10.1109/TII.2011.2166777]

Chen, S.X., An, B., 2010. Time Performance Research on Field Bus Based CNC System. Proc. 2nd ICMEE, p.56-59. [doi:10.1109/icmee.2010.5558489]

Decotignie, J.D., 2005. Ethernet-based real-time and industrial communications. *Proc. IEEE*, **93**(6):1102-1117. [doi:10.1109/JPROC.2005.849721]

Erwinski, K., Paprocki, M., Grzesiak, L.M., Karwowski, K., Wawrzak, A., 2013. Application of Ethernet Powerlink for communication in a Linux RTAI open CNC system. *IEEE Trans. Ind. Electron.*, **60**(2):628-636. [doi:10.1109/TIE.2012.2206348]

Felser, M., 2005. Real-time Ethernet—industry prospective. *Proc. IEEE*, **93**(6):1118-1129. [doi:10.1109/JPROC.2005.849720]

Ferrari, P., Flammini, A., Vitturi, S., 2006. Performance analysis of PROFINET networks. *Comput. Stand. Interf.*, **28**(4):369-385. [doi:10.1016/j.csi.2005.03.008]

Ferrari, P., Flammini, A., Rinaldi, S., Sisinni, E., 2010. On the seamless interconnection of IEEE1588-based devices using a PROFINET IO infrastructure. *IEEE Trans. Ind. Inf.*, **6**(3):381-392. [doi:10.1109/TII.2010.2051954]

FF-581:2003. Fieldbus Foundation System Architecture Specification. Fieldbus Foundation, Austin, TX.

Gaderer, G., Loschmidt, P., Sauter, T., 2010. Improving fault tolerance in high-precision clock synchronization. *IEEE Trans. Ind. Inf.*, **6**(2):206-215. [doi:10.1109/TII.2010.2044580]

Gao, T., Yu, D., Vue, D., Hu, Y., 2010. Design and Implementation of Communication Platform in CNC System. Proc. IEEE/ASME Int. Conf. on MESA, p.355-360. [doi:10.1109/MESA.2010.5552046]

Hanzalek, Z., Burget, P., Sucha, P., 2010. PROFINET IO IRT message scheduling with temporal constraints. *IEEE Trans. Ind. Inf.*, **6**(3):369-380. [doi:10.1109/TII.2010.2052819]

Hespanha, J.P., Naghshtabrizi, P., Xu, Y.G., 2007. A survey of recent results in networked control systems. *Proc. IEEE*, **95**(1):138-162. [doi:10.1109/JPROC.2006.887288]

Hong, S.H., Song, S.M., 2008. Transmission of a scheduled message using a foundation Fieldbus protocol. *IEEE Trans. Instrum. Meas.*, **57**(2):268-275. [doi:10.1109/TIM.2007.910100]

IEC 61158-3, 4, 5, 6:2000. Digital Data Communications for Measurement and Control - Parts 3 to 6: Fieldbus for Use in Industrial Control Systems. IEC, Geneva, Switzerland.

IEC 61784-1:2007. Industrial Communication Networks - Part 1: Digital Data Communications for Measurement and Control - Part 1: Profile Sets for Continuous and Discrete Manufacturing Relative to Fieldbus Use in Industrial Control Systems. IEC, Geneva, Switzerland.

IEC 61784-2:2007. Digital Data Communications for Measurement and Control - Part 2: Additional Profiles for ISO/IEC8802-3 Based Communication Networks in Real-Time Applications. IEC, Geneva, Switzerland.

IEC 61784-14:2007. Industrial Communication Networks - Part 14: Additional Fieldbus Profiles for Real-Time Networks Based on ISO/IEC 8802-3. IEC, Geneva, Switzerland.

IEEE 1588:2008. Precision Clock Synchronization Protocol for Networked Measurement and Control Systems.

IEEE 802.3:2005. Carrier Sense Multiple Access with Collision Detection (CSMA/CD) Access Method and Physical Layer Specifications.

Jasperneite, J., Schumacher, M., Weber, K., 2007. Limits of Increasing the Performance of Industrial Ethernet Protocols. IEEE Conf. on Emerging Technologies & Factory Automation, p.17-24. [doi:10.1109/EFTA.2007.4416748]

Kim, K., Sung, M., Jin, H.W., 2012. Design and implementation of a delay-guaranteed motor drive for precision motion control. *IEEE Trans. Ind. Inf.*, **8**(2):351-365. [doi:10.1109/TII.2011.2166774]

Monmasson, E., Idkhajine, L., Cirstea, M.N., Bahri, I., Tisan, A., Naouar, M.W., 2011. FPGAs in industrial control applications. *IEEE Trans. Ind. Inf.*, **7**(2):224-243. [doi:10.1109/TII.2011.2123908]

Prytz, G., 2008. A Performance Analysis of EtherCAT and PROFINET IRT. IEEE Conf. on Emerging Technologies & Factory Automation, p.408-415. [doi:10.1109/EFTA.2008.4638425]

Raja, P., Ruiz, L., Decotignie, J.D., 1994. Modeling and Scheduling Real-Time Control Systems with Relative Consistency Constraints. Proc. 6th Euromicro Workshop on Real-Time Systems, p.46-52. [doi:10.1109/EMWRTS.1994.336866]

Sauter, T., 2007. The continuing evolution of integration in manufacturing automation. *IEEE Ind. Electron. Mag.*, **1**(1):10-19. [doi:10.1109/MIE.2007.357183]

Sauter, T., 2010. The three generations of field-level networks—evolution and compatibility issues. *IEEE Trans. Ind. Electron.*, **57**(11):3585-3595. [doi:10.1109/TIE.2010.2062473]

Sauter, T., Vasques, F., 2006. Special section on communication in automation. *IEEE Trans. Ind. Inf.*, **2**(2):73-77. [doi:10.1109/TII.2006.875801]

Schumacher, M., Jasperneite, J., Weber, K., 2008. A New Approach for Increasing the Performance of the Industrial Ethernet System PROFINET. IEEE Int. Workshop on Factory Communication Systems, p.159-167. [doi:10.1009/WFCS.2008.4638725]

van den Heuvel, M.M.H.P., Bril, R.J., Lukkien, J.J., 2012. Transparent synchronization protocols for compositional real-time systems. *IEEE Trans. Ind. Inf.*, **8**(2):322-336. [doi:10.1109/TII.2011.2172448]

Vitturi, S., Peretti, L., Seno, L., Zigliotto, M., Zunino, C., 2011. Real-time Ethernet networks for motion control. *Comput. Stand. Interf.*, **33**(5):465-476. [doi:10.1016/j.csi.2011.01.005]